layers. We reproduced the bias voltage dependence of light emission with a substantially lesser signal-to-noise ratio, yet with a comparable photon yield per tunneling electron. This light-emitting junction, even at its current incarnation, has an imaging area that is notably smaller than that of the best optical microscope, comparable to that of near field microscopes. Our main goal, however, is to image individual adsorbed chromophore molecules by monitoring their light emission images in STM. Unlike transmission electron microscopy or x-ray diffraction, our method could be performed in the natural (that is, aqueous) environment, "highlighting" specific chemical groups.

REFERENCES AND NOTES

1. P. Avouris, *J. Phys. Chem.* **94**, 2246 (1990).
2. R. J. Hammers, R. M. Tromp, J. E. Demuth, *Phys. Rev. Lett.* **56**, 1972 (1986).
3. S. Chiang, in *Scanning Tunneling Microscopy I*, H. J. Guntherodt and R. Wiesendanger, Eds. (Springer-Verlag, Berlin, 1992), pp. 181–205.
4. D. P. E. Smith, M. D. Kirk, C. F. Quate, *J. Chem. Phys.* **86**, 6034 (1987).
5. D. W. Pohl, in *Scanning Tunneling Microscopy II*, R. Wiesendanger and H. J. Guntherodt, Eds. (Springer-Verlag, Berlin, 1992), pp. 233–271.
6. K. Lieberman, S. Harush, A. Lewis, R. Kopelman, *Science* **247**, 59 (1990).
7. J. K. Gimzewski, B. Reihl, J. H. Coombs, R. R. Schlittler, *Z. Phys. B* **72**, 497 (1988).
8. R. Berndt and J. K. Gimzewski, *Phys. Rev. B* **45**, 14095 (1992).
9. ——— and P. Johansson, *Phys. Rev. Lett.* **67**, 3796 (1991).
10. R. Berndt, J. K. Gimzewski, R. R. Schlittler, *Z. Phys. D* **26**, S87 (1993).
11. B. N. J. Person and J. E. Demuth, *Solid State Commun.* **57**, 769 (1986).
12. A. Campion, A. R. Gallo, C. B. Harris, H. J. Robota, P. M. Whitemore, *Chem. Phys. Lett.* **73**, 447 (1980).
13. P. Avouris and B. N. J. Persson, *J. Phys. Chem.* **88**, 837 (1984).
14. K. L. Chopra, S. Major, K. Pandya, *Thin Solid Films* **102**, 1 (1983).
15. P. K. Hansma, *IBM J. Res. Dev.* **30**, 370 (1986).
16. We acknowledge useful discussions with M. Levin, J. Jortner, and U. Even.

7 June 1993; accepted 25 October 1993

Fabrication of Conducting Polymer Interconnects

Corrine L. Curtis, Jason E. Ritchie, Michael J. Sailor*

A nonmechanical approach to the construction of complex three-dimensional interconnect arrays has been developed with the use of conducting polymer dendrites. Electrically independent connections between pairs of wires in an array were successfully grown through alternating-current electrochemical polymerization of poly(3-methylthiophene), without mechanical or optical masking steps. The electrically active links were insulated by subsequent electropolymerization of 4-vinylpyridine or 2-methylthiophene or by the dip-coating of the connections in a polystyrene solution.

A major obstacle in the development of nanoscale fabrication techniques lies in the increasing difficulty of manipulating three-dimensional (3D) structures as their sizes decrease. For molecular electronics or artificial neural networks, the number and size of the interconnects required makes the fabrication of structures with >100 nodes difficult (*1*–*6*). A structure as complicated as the human brain, which contains ~10^{12} nodes (neurons) and a thousand times that many interconnecting links (*7*), would be virtually impossible to fabricate with conventional mechanical or photolithographic techniques (*8*). The use of chemical procedures to direct the linking of "molecular wires" such as conducting organic polymer strands has been recognized as a potentially viable approach for some time, and progress has been made in this direction (*9*–*16*). However, a general technique for connecting a large number of such molecular wires independent of each other has not been discovered.

In this report, we demonstrate an electrochemical polymerization technique that allows for the interconnection of many individual Pt nodes in three dimensions. The technique takes advantage of the ability of conductive polymers such as poly(3-methylthiophene) (P3MT) to be electrochemically switched between electronically conducting and nonconducting states. These polymers only grow when they are in their conducting form. We show that a pair of selected Pt wires can be electrically linked with polymer dendrites by the passing of an alternating current between them. The polymer dendrites alternate between conducting and nonconducting states until they come into contact with each other. When an actively polymerizing strand electrically contacts a nonconductive strand, the nonconductive strand switches into its conductive state in the region close to the connection. Further polymerization then occurs in the contacted region to reinforce the connection. The process requires no external mechanical manipulation or lithographic patterning. By the use of a separate insulation step, sets of nodes can be prepared that are electrically independent of each other.

A square array of four Pt wires was mounted in epoxy, each equidistant (~2 mm) from the others. These four "nodes" served as the working electrodes, and a fifth Pt wire coated with doped P3MT was used as a reference electrode. A counter electrode (Pt strip, 1-cm^2 area) was mounted in a compartment separated from the Pt wire array by a sintered glass filter. The polymerization solutions consisted of 3-methylthiophene (0.17 M) and tetrabutylammonium tetrafluoroborate (between 0.1 and 0.025 M) in dry, deoxygenated acetonitrile (*17*). Two of the four Pt nodes were connected to a bipotentiostat setup as independent working electrodes, with a common reference electrode (*18*). The potentials at the two nodes were scanned (triangular waveform, 100 mV/s) from −0.5 to +1.7 V relative to the reference electrode potential. The triangular waveform at one electrode was inverted with respect to the other, so that when either node was at −0.5 V the other was at +1.7.

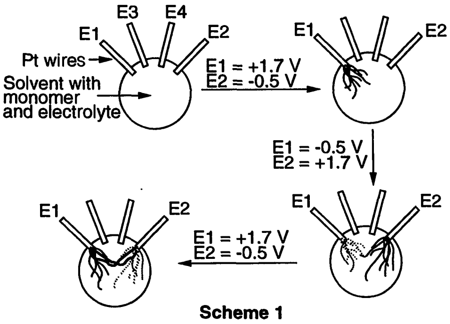

Scheme 1

The rationale for the conducting polymer connection technique is outlined in Scheme 1. The accepted mechanism for electropolymerization of 3-alkylthiophenes involves the oxidative coupling of thiophene rings primarily at the 2 position (*19*). Concomitant with the polymerization reaction is the partial oxidation of the polymer chain, which dopes the polymer into an electronically conducting state. Thus, when the potential on one of the Pt leads (E1 in Scheme 1) is +1.7 V, polymerization and chain growth occurs. Under the conditions of the present experiments, the growth morphology is dendritic, and so fibers of P3MT propagate into solution (Fig. 1). The potential at the original Pt node (E1 in Scheme 1) is then scanned in the negative direction as the potential of a second Pt node (E2) is scanned positive, relative to the reference electrode. The polymer dendrites attached to the first node

---

Department of Chemistry, University of California, San Diego, La Jolla, CA 92093–0358.

*To whom correspondence should be addressed.

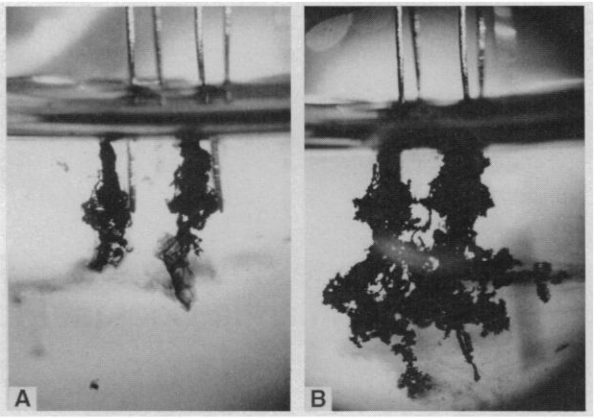

Fig. 1. Optical photographs of a polymerization sequence connecting two of four Pt nodes: (**A**) initial polymerization stages and (**B**) at the point that polymer connection is established between the two wires. The wires are spaced 2 mm apart.

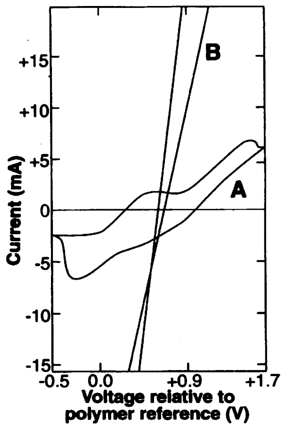

Fig. 2. Current-voltage curves measured at one of the Pt nodes (**A**) before polymer connection, showing the doping, polymerization, and undoping waves; and (**B**) after connection to another wire, showing the current-voltage wave characteristic of an electronic shunt.

(E1) become undoped and nonconductive, whereas new dendrites nucleate and grow at the second Pt node (E2). This process continues in an alternating fashion until a dendrite from one Pt node comes into physical contact with a dendrite from the other Pt node. At this stage, the polymer can act as an electrical shunt between the two Pt leads. As a shunt, the voltage drop in any segment of the polymer link is proportional to the resistance of that segment. Oxidized, actively polymerizing P3MT is approximately eight orders of magnitude more conductive than the reduced form (*20*, *21*). Thus, when one Pt wire is at +1.7 V, the voltage along most of the length of a connected polymer link tends to be maintained at close to +1.7 V and then drops rapidly to −0.5 V near the Pt wire that is at −0.5 V. As the potential scans, this situation inverts, with the net effect that most of the polymer connection is maintained at a voltage positive of the doping and polymerization potential. The system keeps the newly attached dendrite in the oxidized state, where further electropolymerization can take place and reinforce the connection. The above interpretation assumes that the potential scan rate is slow relative to the rates of doping and undoping.

The current-voltage transients monitored at either Pt node (Fig. 2) were consistent with the above mechanism. During the initial polymerization stages, the growing polymer dendrites displayed current-voltage transients characteristic of the thiophene-polythiophene electrochemical system (Figs. 1A and 2A) (*22*). Distinct waves were observed for anodic polymerization and doping currents at potentials of +0.5 and +1.5 V (relative to doped P3MT), respectively, and for the cathodic undoping current at −0.3 V (Fig. 2A). After several minutes, the slope of the current-voltage curve increased dramatically, signifying that the polymeric shunt connecting the two Pt leads had been established (Figs. 1B and 2B). At this point, the electrical conductivity between the two Pt nodes was determined by a two-electrode measurement of the current-voltage curve (over a range of ±5 mV) between the two nodes. In most cases, conductivity between the two nodes was retained when the assembly was removed from the polymerization solution and allowed to dry.

To test the feasibility of this technique to establish multiple, independent 3D connections, a second link was subsequently electropolymerized between two additional Pt nodes. To avoid cross talk between the two connections, an insulating layer was added to the first polymer link before electropolymerization at the second pair of Pt wires. Two insulation techniques were attempted. The first involved the electropolymerization of either poly(2-methylthiophene) or poly(4-vinylpyridine), which were both found to insulate the existing P3MT connection (*19*, *23*). The insulators were polymerized in a separate propylene carbonate or acetonitrile solution. The second insulation technique involved the dipping of the doped polymer connection into a tetrahydrofuran solution of polystyrene (which contained a small amount of plasticizer).

After insulation of the first set of nodes, a second interconnect was electropolymerized at nodes corresponding to E3 and E4 of Scheme 1. For the dip-coated samples, polymerization at the second set of nodes was sometimes initiated by the momentary stepping of the electrode potentials of E3 and E4 to +5 V, to break down the residual polystyrene layer on the Pt leads. The resistance between two connected nodes typically ranged from 8 to 450 ohms, while the resistance between independent insulated nodes (cross talk) was up to 36 times greater (Table 1). The insulating procedures were not always successful, presumably because of cracking of the insulator films during the processing steps. Insulation by electropolymerization was less consistent than the dip-coating method.

Table 1. Resistance data for four Pt nodes from 10 separate experiments. Poly(3-methylthiophene) connection was made between nodes E1 and E2 first, then between nodes E3 and E4. Resistances were measured in situ. Cross talk is the measured resistance between the indicated nodes. The insulator used for these runs (on nodes E1 and E2) was polystyrene.

Trial	E1-E2 (ohms)	E3-E4 (ohms)	Cross talk (ohms)			
			E1-E3	E1-E4	E2-E3	E2-E4
1	74.9	69.9	551	474	556	508
2	30.1	168	636	876	711	766
3	14.1	88.2	1100	1200	939	941
4	11.6	7.87	138	130	141	140
5	9.20	77.5	205	654	172	1104
6	8.10	359	1080	59.5	738	62
7	14.7	44.7	943	938	962	952
8	8.85	135	1940	1890	1840	1910
9	13.7	442	18000	20000	16000	20000
10	9.85	62.7	202	163	189	185

The polymer connections display several properties that may be relevant to the neural network, fuzzy logic, or other nanofabricated model systems. Information is contained in a link in the form of a net conductivity value. The duty cycle, polymerization time, and potential limits used in the process determine this conductivity, and so a wide range of "connection strengths" is accessible. The technique is not limited to a single pair of nodes. In theory, a large number of nodes could be connected in common, with varying connection strengths again determined by the conductivity between each node and the common pool. Because the conductivity of conducting polymers can range over eight orders of magnitude, the polymer networks can store a large amount of information in a relatively small volume. A link formed by electropolymerization can be made to "forget" if the potential of all of its nodes is held negative of the polymer doping potential while the array is immersed in an electrolyte solution. We have observed that under these conditions, the polymer link undopes and becomes insulating, as expected from established polythiophene electrochemistry (*20, 21*). The link can be "reminded" again if the array potential is adjusted positive of the doping potential. This doping-undoping electrochemistry is a way of storing information in the form of a conductivity value. Although this method may be an advantage relative to current 2D optical or magnetic storage devices, the polymer doping process relies on ion migration and so is expected to be inherently slower than devices that use electron transport processes (such as conventional Si-based random-access memory chips).

REFERENCES AND NOTES

1. W.-J. Sah, S.-C. Lee, H.-K. Tsai, J.-H. Chen, *Appl. Phys. Lett.* **56**, 2539 (1990).
2. M. A. Sivilotti, M. R. Emerling, C. A. Mead, *AIP Conf. Proc.* **151**, 408 (1986).
3. J. J. Hopfield, J. N. Onuchic, D. N. Beratan, *J. Phys. Chem.* **93**, 6350 (1989).
4. H. P. Graf *et al.*, *AIP Conf. Proc.* **151**, 182 (1986).
5. J. Alspector, *IEEE Commun. Mag.* **11**, 29 (1989).
6. D. Psaltis, D. Brady, X.-G. Gu, S. Lin, *Nature* **343**, 325 (1990).
7. S. W. Kuffler and J. G. Nichols, *From Neuron to Brain* (Sinauer, Sunderland, MA, 1976), p. 7.
8. T. Nordstrom and B. Svensson, *J. Parallel Distrib. Comput.* **14**, 260 (1992).
9. S. Li, C. W. Macosko, H. S. White, *Science* **259**, 957 (1993).
10. J. H. Kaufman, C. K. Baker, A. I. Nazzal, M. Flickner, O. R. Melroy, *Phys. Rev. Lett.* **56**, 1932 (1986).
11. R. J. v. Gutfeld and D. R. Vigliotti, *Appl. Phys. Lett.* **56**, 2584 (1990).
12. T. Kawai, H. Motobayashi, T. Kuwabara, K. Yoshino, *Jpn. J. Appl. Phys.* **30**, L622 (1991).
13. J. J. Hickman *et al.*, *J. Am. Chem. Soc.* **111**, 7271 (1989).
14. J. J. Hickman *et al.*, *Langmuir* **8**, 357 (1992).
15. C. H. McCoy and M. S. Wrighton, *Chem. Mater.* **5**, 914 (1993).
16. G. P. Kittlesen, H. S. White, M. S. Wrighton, *J. Am. Chem. Soc.* **106**, 7389 (1984).
17. D. F. Shriver and M. A. Drezdzon, *The Manipulation of Air-Sensitive Compounds* (Wiley, New York, ed. 2, 1986), pp. 90–91.
18. A. J. Bard and L. R. Faulkner, *Electrochemical Methods* (Wiley, New York, 1980), p. 301.
19. G. Tourillon, *Handbook of Conducting Polymers*, T. A. Skotheim, Ed. (Dekker, New York, 1986), vol. 1, pp. 293–350.
20. K. Kaneto, K. Yoshino, Y. Inuishi, *Solid State Commun.* **46**, 389 (1983).
21. G. Tourillon and F. Garnier, *J. Phys. Chem.* **87**, 2289 (1983).
22. T. F. Otero and E. d. Larreta-Azelain, *Polymer* **29**, 1522 (1988).
23. H. O. Finklea and R. S. Vithanage, *J. Electroanal. Chem.* **161**, 283 (1984).
24. We thank P. Asbeck for helpful discussions and the U.S. Department of Education for a Graduate Assistance in Areas of National Need Graduate Fellowship (C.L.C.). Supported in part by an Office of Naval Research grant and by the Donors of the Petroleum Research Fund.

10 August 1993; accepted 3 November 1993

Stable Isotope Enrichment in Paleowaters of the Southeast Atlantic Coastal Plain, United States

L. Niel Plummer

Paleowaters from the Floridan aquifer system in the southeastern Atlantic coastal plain have higher D/H and $^{18}O/^{16}O$ ratios than local Holocene ground water. Maximum $\delta^{18}O$ enrichments in ground water having adjusted radiocarbon ages of 20,000 to 26,000 years are 0.7 to 2.3 per mil. The trend in isotopic enrichment in paleowaters is the reverse of that normally observed in continental glacial age ground water. Dissolved nitrogen and argon concentrations indicate, however, that the average recharge temperature was 5.3°C cooler than that today. The data indicate cool conditions in the southeast Atlantic coastal plain during the last glacial maximum, with recharge limited primarily to late summer tropical cyclones and hurricanes.

Ground water recharged during the last glacial maximum (LGM) is recognized worldwide by depletion in D and ^{18}O in comparison to Holocene ground water (*1–5*). This is attributed to isotopic fractionation as atmospheric moisture condenses in colder climates and, in some cases, to recharge from melting ice (*6*). For example, isotopically depleted paleowaters recharged during the LGM in central Europe indicate that temperatures were 7°C less than in Holocene times (*3*). Noble gas measurements (*7*) support the stable isotope data and are consistent with values of the stable isotope temperature coefficient, $\Delta\delta^{18}O/\Delta T$, of 0.40 to 0.70 per mil per degree Celsius (*4, 7–9*).

Studies of stable isotope depletion in European paleowaters have found no evidence that the continental temperature gradient differed between modern and glacial times (*3*). Therefore, it has been assumed that water vapor transport patterns over Europe were little changed in the last ice age and that the average degree of rain out of air masses was similar to the present (*3*).

In the southwest and south-central United States, stable isotope depletion and noble gas measurements in paleowaters indicate that temperatures were 5° to 7°C less than those in the late Wisconsin (*5, 10–12*). Pollen studies and other fossil records in the southeast United States also indicate a cooling of 5° to 7°C during the LGM (*13, 14*). In contrast, climate model results (*15–18*) indicate a cooling of only a few degrees in both January and July temperatures in the Gulf of Mexico surface waters at the LGM. Both model predictions (*15–17*) and pollen records from lake sediments (*19*) indicate significantly dryer conditions in the southeast United States during the LGM.

This report describes isotopically enriched paleowaters in the Floridan aquifer system of the southeast Atlantic coastal plain, United States, and compares these data with paleorecharge temperatures determined from measurements of dissolved gases. Together, these data can be used to evaluate climatic conditions and atmospheric circulation patterns in the southeastern United States during the LGM (*20*).

The hydrology and chemistry of the Floridan aquifer system has been extensively studied (*21–23*). In north-central Georgia, the aquifer system crops out as thin sand and marl of Tertiary age that thicken into limestone and dolostone to the southeast and east. The aquifer system is 600 m, and locally 800 m, thick along the Atlantic coast. The Floridan aquifer system is locally subdivided into two permeable zones, the Upper and Lower Floridan aquifers, separated by a dolomite. The Upper Floridan aquifer is typically 90 to 180 m thick in Georgia and is overlain by 90 to 180 m of low-permeability Miocene sediment, which forms the upper confining unit.

The Floridan aquifer system is underlain by Cretaceous and Tertiary clastic sedimentary rocks that generally thicken to the southeast. In Georgia, these underlying rocks are subdivided into three regional aquifers separated by confining units (*24*). The uppermost clastic regional aquifer (A2, or Gordon aquifer) is hydraulically con-

---

U.S. Geological Survey, Reston, VA 22092.